

Age of the emerald mineralization from the Itabira-Nova Era District, Minas Gerais, Brazil, based on LA-ICP-MS geochronology of cogenetic titanite

Idade da mineralização de esmeralda do distrito de Itabira-Nova Era, Minas Gerais, Brasil, com base em geocronologia LA-ICP-MS de titanita cogenética

Hanna Jordt-Evangelista^{1*}, Cristiano Lana¹,
Carlos Eduardo Reinaldo Delgado¹, Deiwys José Viana¹

ABSTRACT: In the Itabira-Nova Era Emerald District, southeast Brazil, gemological emerald is extracted from underground mines found in schist-type deposits at the contact zone of the Archean Metavolcanosedimentary Sequence of the Guanhães Complex and Paleoproterozoic anorogenic granites of the Borrachudos Suite. Schist-type deposits are commonly generated by reactions enhanced by deformation and heat during regional metamorphism. The age of the mineralization in the region has been a matter of debate for decades: Ages ranging from the Archean to the Neoproterozoic are mentioned in the literature. In the mineralized zone from the Piteiras mine fluorine-aluminum-bearing titanite is found in metamafic rocks. The fluorine content was probably derived from the Borrachudos granites and pegmatites like the beryllium for emerald, thus both minerals could have been generated during the same event. U-Pb titanite geochronology via laser ablation inductively coupled plasma mass spectrometry (LA-ICP-MS) was performed on a thin section of a phlogopite-plagioclase-hornblende schist from the Piteiras mine. The determined age of 576 ± 7 Ma is also the probable age for emerald generation during the Brasiliano cycle, which was the only tectonometamorphic event postdating the intrusion of the granites. This event provided heat and fluids necessary for reactions between the Be- and the Cr-bearing rocks, thus enabling the formation of emeralds.

KEYWORDS: Titanite, U/Pb geochronology, Neoproterozoic, Emerald, Brazil.

RESUMO: No Distrito Esmeraldífero de Itabira-Nova Era, sudeste do Brasil, esmeralda gemológica é extraída em minas subterrâneas em depósitos do Tipo Xisto na zona de contato da sequência metavulcanosedimentar arqueana do Complexo Guanhães com granitos anorogênicos paleoproterozoicos da Suite Borrachudos. Depósitos do Tipo Xisto são comumente gerados por reações promovidas por deformação e calor durante metamorfismo regional. A idade da mineralização na região tem sido motivo de debates por décadas: idades variando do Arqueano ao Neoproterozoico são mencionadas na literatura. Na zona mineralizada da mina Piteiras, titanita portadora de alumínio e flúor é encontrada em rochas metamáficas. O conteúdo de flúor foi provavelmente derivado dos granitos e pegmatitos Borrachudos, tal como o berílio para a esmeralda, portanto ambos minerais podem ter sido gerados durante o mesmo evento. Geocronologia U-Pb via ablação a laser associada a espectrometria de massa por plasma acoplado indutivamente a laser (LA-ICP-MS) em titanita foi realizada em uma seção delgada de um flogopita-plagioclásio-hornblenda xisto da mina Piteiras. A idade determinada de 576 ± 7 Ma é também a provável idade de geração da esmeralda durante o ciclo Brasiliano, que foi o único evento tectonometamórfico posterior à intrusão dos granitos. Este evento forneceu calor e fluidos necessários para reações entre as rochas portadoras de berílio e de cromo, possibilitando assim a formação de esmeralda.

PALAVRAS CHAVE: Titanita, geocronologia U/Pb, Neoproterozoico, Esmeralda, Brasil.

¹Departamento de Geologia, Escola de Minas, Universidade Federal de Ouro Preto (UFOP) – Ouro Preto (MG), Brazil. E-mails: hanna@degeo.ufop.br, cristianoDECLANA@gmail.com, delgado@geologist.com, deiwysviana@gmail.com

*Corresponding author.

Manuscript ID: 20160074. Received In: 06/13/2016. Approved In: 06/14/2016.

INTRODUCTION

The formation of emeralds requires the uncommon interaction of beryllium and chromium, the latter being the usual chromophore element responsible for the typical green color. Be and Cr are incompatible elements found in quite distinct geochemical environments; while Be is concentrated in granitic rocks and their pegmatites, higher amounts of Cr are mostly found in mafic, and especially ultramafic igneous rocks. In order to enable the formation of emerald, reactions between these two contrasting lithotypes are usually enhanced by deformation. Among the emerald deposits found worldwide, the schist type is one of the most important. The reactions involved in the formation of this type of deposit usually happen during a tectonometamorphic event since the simple intrusion of granites or pegmatites in ultramafic rocks is not able to supply enough energy and fluids to produce important reaction zones (Franz *et al.* 1996, Franz & Morteani 2002). As suggested by Grundmann and Morteani (1989), most if not all schist-type emerald deposits in metamorphic rocks may be the product of a deformational

event accompanied or followed by regional metamorphism which provided heat and the abundant fluids necessary for the reactions of Be- and Cr-rich rocks. In addition, the transformation of the original ultramafic rock (peridotites and/or their volcanic equivalents such as komatiites) into the typical emerald-bearing phlogopite schists is due to the percolation of K-rich fluids derived from pegmatites under the influence of deformation.

The Itabira-Nova Era Emerald District (Fig. 1), located ca. 120 km northeast of Belo Horizonte, state of Minas Gerais, Brazil, is known worldwide for the production of high-quality emerald gems. The two main mines, Belmont and Capoeirana, besides the temporarily closed mines Piteiras and Rocha, are found at the contact zone of metaultramafic phlogopite schists of the Metavolcanosedimentary Sequence correlative of the Archean Guanháes Complex (Padilha *et al.* 2000) and the Paleoproterozoic anorogenic Borrachudos granites (Dorr and Barbosa 1963, Grossi-Sad *et al.* 1990, Dossin *et al.* 1993, Chemale Jr. *et al.* 1997, Silva *et al.* 2002). Souza (1988), Giuliani *et al.* (1990), Souza *et al.* (1992), Machado (1998), Schwarz and Giuliani (2001), Schwarz

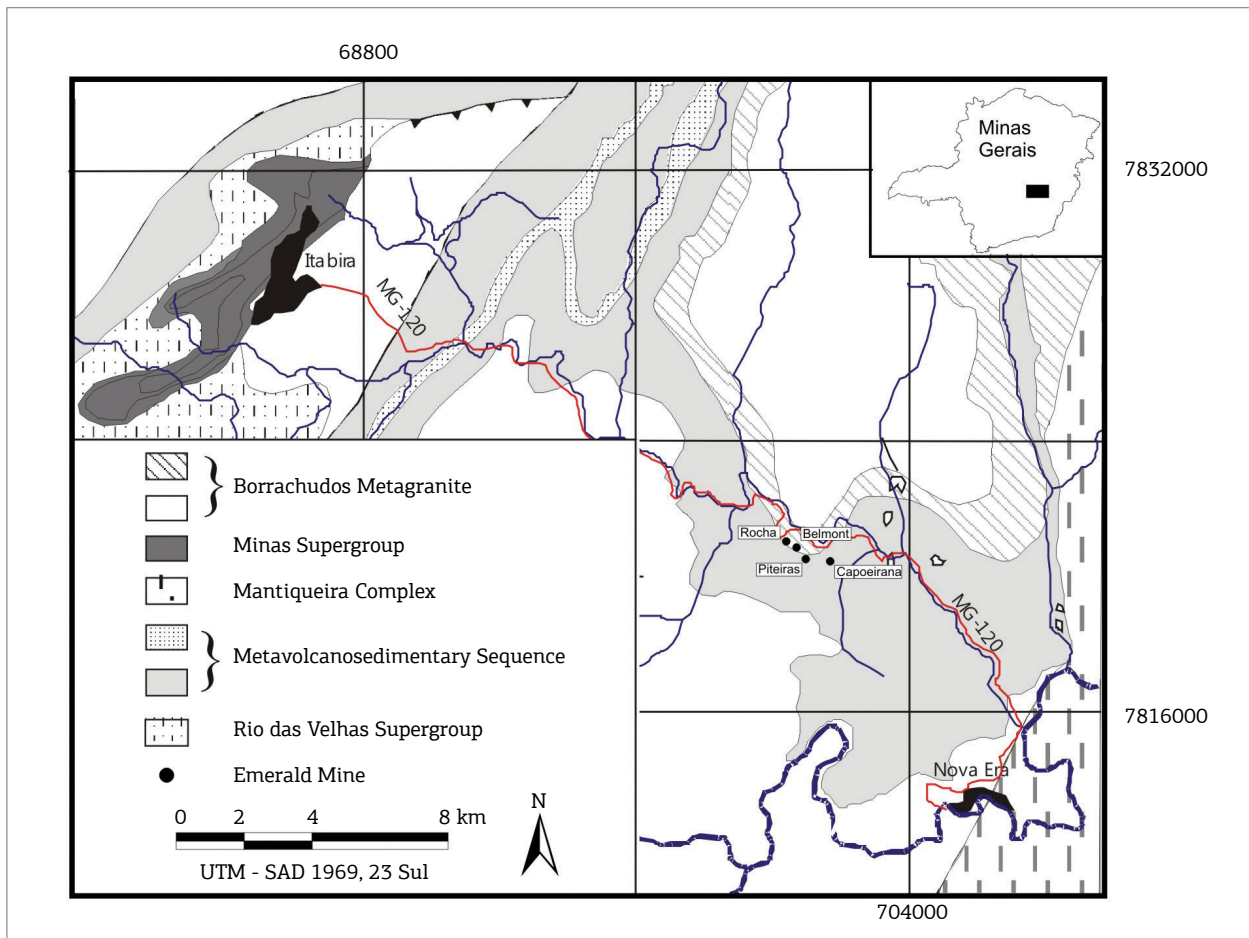


Figure 1. Simplified geological map of the area of the Itabira-Nova Era Emerald District (modified from Machado 1998) and the location of the emerald mines Piteiras, Belmont, Rocha, and Capoeirana.

et al. (2002), and Franz and Morteani (2002) have classified the deposits of Belmont and Capoeirana as belonging to the schist type. Similar studies by Viana (2004), Viana *et al.* (2006), and Delgado (2007) in the mines Piteiras and Rocha led to the conclusion that also in these mines the emerald deposit is of identical origin.

The age of the schist-type mineralization in the Itabira-Nova Era Emerald District remains debatable. More than one phase of mineralization was described by some authors based on the observation of two types of emeralds: one strongly deformed and therefore considered as older, and another undeformed and therefore postulated as being younger (Machado 1994, 1998, Ribeiro-Althoff *et al.* 1997, Morteani *et al.* 2000, Preinfalk *et al.* 2002, Ribeiro 2006). Schorscher (1991), Machado (1994, 1998), and Ribeiro (2006) interpreted the strongly deformed generation as of Archean age and the underformed generation as being Proterozoic. However, if the growth of emeralds lasts during the whole time span of a tectonometamorphic event, the early-formed crystals would be deformed while the late crystals remain undeformed. Considering that the mineralization is controlled by the spatial association of the Archean Metavolcanosedimentary Sequence with the Paleoproterozoic Borrachudos granite plutons and their pegmatites, the mineralization cannot be Archean. A Paleoproterozoic age for the mineralization was postulated by Preinfalk *et al.* (2002) based on Rb-Sr dating of pegmatites associated with the Borrachudos anorogenic metagranitoids. If, as discussed earlier, the generation of schist-type mineralization is associated with a tectonometamorphic event, the emerald formation in the region of Itabira-Nova Era cannot be of the same age as the 1.7 Ga Borrachudos magmatism because at that time the Transamazonian (~2.0 Ga) tectonometamorphic event had already ceased. The only major tectonometamorphic event in the region postdating the intrusion of the Borrachudos granites is the Brasiliano event (~0.7 – 0.5 Ga) that could therefore be responsible for the emerald generation.

In order to check if the Brasiliano tectonometamorphic event played a role during the generation of the schist-type emerald mineralization, this paper presents the results of *in situ* laser ablation inductively coupled plasma mass spectrometry (LA-ICP-MS) U-Pb age determination on metamorphic fluorine-aluminum-bearing titanite belonging to a metamafic schist found in the mineralized zone from the Piteiras mine. The generation of both titanite and emerald was probably synchronous, therefore the age of the titanite is relevant to establish the age of the mineralization.

Geological Setting

The Itabira-Nova Era emerald deposits belong to the Santa Maria de Itabira Pegmatite District (Netto *et al.* 1998),

in the southern portion of the Eastern Brazilian Pegmatite Province (Paiva 1946, Correia Neves *et al.* 1986). The deposits are located near the northeastern border of the Quadrilátero Ferrífero (QF), which is an important province for gold and iron deposits (Dorr 1969).

The oldest rocks of Archean age of this region record the influence of two younger orogenic events, the Transamazonian (~2 Ga) and the Brasiliano (0.7 – 0.5 Ga; Brito Neves & Cordani 1991, Alkmim and Marshak 1998). The strong influence of the Brasiliano event in the region of Itabira-Nova Era is recorded in the regional structures described by Peres *et al.* (2004) and Padilha *et al.* (2000) as well as in geochronological data by Ribeiro-Althoff *et al.* (1997), Fernandes *et al.* (2000), and Preinfalk *et al.* (2002).

The geological outline in the Itabira-Nova Era region (Fig. 1) is defined by the envelopment of metagranitic plutons of the Paleoproterozoic Borrachudos Suite (Grossi-Sad *et al.* 1990) by rocks of the Metavolcanosedimentary Sequence correlative of the Archean Guanhães Complex (Padilha *et al.* 2000). The emerald mineralization is found mainly at this contact zone. Rocks belonging to the Archean Rio das Velhas greenstone belt, and to the Paleoproterozoic Minas Supergroup and Mantiqueira Complex are found locally. Additional lithotypes are younger metamafic bodies and the pegmatites associated with the emerald mineralization.

Although gneisses and metagranitoids are prevalent in the area, there is no consensus about their spatial arrangement and stratigraphic relationship; thereby the crystalline basement has been recorded in the literature as belonging to the Guanhães or to the Mantiqueira complexes. Souza (1988) and Schorscher (1991) named the rocks of the crystalline basement as Archean TTG Complex. The lithotypes of the Metavolcanosedimentary Sequence are metaultramafic, metamafic, and metasedimentary rocks that occur as meter-sized intercalations within TTG gneisses and migmatites dated at 2.9 – 2.7 Ga (U/Pb SHRIMP age, Silva *et al.* 2002). In the area of the emerald mines, the metaultramafic rocks host the emerald mineralization.

The main lithotypes of the Mantiqueira Complex are banded and locally migmatized orthogneisses of granitic, granodioritic, and tonalitic composition. Lenses of amphibolites are relatively common. U-Pb SHRIMP age determinations resulted in Paleoproterozoic magmatic crystallization ages of 2.21 – 2.05 Ga and metamorphic ages of 2.05 Ga and of 560 Ma (Silva *et al.* 2002).

Sericitic and ferruginous quartzite and phyllite, banded iron formations, and marble are the rock types of the Minas Supergroup in the Itabira-Nova Era region.

Metagranitic bodies of the Borrachudos Suite make up most of the area in Figure 1. They are composed of anorogenic alkaline metagranites related to the opening of the

Espinhaço rift (Chemale Jr. 1987, Fernandes *et al.* 1995, Chemale Jr. *et al.* 1997, Dussin *et al.* 1997, Silva *et al.* 2002). Shear zones leading to variable degrees of gneissification are common (Peres *et al.* 2004). Quartz, microcline, plagioclase (commonly nearly pure albite, Jordt-Evangelista *et al.* 2000) and biotite are the main minerals. Additionally, there are subordinated amounts of hornblende, titanite, apatite, garnet, zircon, ilmenite, and fluorite. Fluorite is a diagnostic mineral for the Borrachudos granitoids, enabling its distinction from the quartz-feldspar-rich rocks belonging to other geological units. Single-zircon dating by stepwise Pb evaporation yielded a Paleoproterozoic crystallization age of 1.7 Ga for the Borrachudos granite (Dussin *et al.* 1993) corroborated by the 1.74 Ga U-Pb SHRIMP age by Silva *et al.* (2002). Neoproterozoic U/Pb ages of 620 Ma on zircon were obtained by Fernandes *et al.* (2000) for the metamorphism and anatexis of the Borrachudos Suite.

Pegmatites occur as veins, dykes, and pods within all rock units of the region. They are mostly composed of albite, less common are quartz, micas, and microcline. Accessory minerals not found in all pegmatites are beryl, apatite, molybdenite, chrysoberyl, monazite, and titanite. Preinfalk *et al.* (2002) dated the pegmatites by the Rb-Sr method and found an older, 1.9 Ga generation, and a younger, dated 480 Ma that is associated with the migmatization of the Borrachudos granite. $^{40}\text{Ar}/^{39}\text{Ar}$ age of 508 ± 2 Ma was determined by Ribeiro-Althoff *et al.* (1997) on biotite from the emerald-bearing biotites at Capoeirana, which was considered as the emerald forming event. However, this Brasiliano age was considered by Preinfalk *et al.* (2002) as the rejuvenation rather than the crystallization age. The formation of a second emerald generation during the Brasiliano event is not excluded by Preinfalk *et al.* (2002).

Piteiras Mine

The country rocks in the Piteiras Mine where the dated titanite sample was collected are centimeter to decimeter thick banded gneisses belonging to the Metavolcanosedimentary Sequence correlative of the Guanhões Complex. They are made up of quartz, plagioclase, biotite, and garnet, less commonly also staurolite, kyanite, and fibrolitic sillimanite. These paragneisses show gradational contacts with biotite gneisses of tonalitic to granodioritic composition. Less commonly layers of quartz-plagioclase-anthophyllite granofels can be found. PT-conditions of the amphibolite facies are indicated by the presence of staurolite. These conditions were corroborated by geothermobarometric calculations which resulted in $T = 610^\circ\text{C}$ and $P = 5.2$ kbar (Viana *et al.* 2006). The emerald mineralization occurs in a 2–4 m thick and hundreds of meters long phlogopite-rich horizon. Due to folding, the thickness may locally reach

12 m. The mineralized metamafic/metaultramafic horizon comprises amphibole-biotite schists enclosing centimeter to meter thick lenses of gneisses similar to the above described country rocks, of amphibole schists (also named ultramafic amphibolites), of amphibolite, and of phlogopite schist. Pegmatites occur as irregular bodies up to 8 m long which may be concordant or discordant in relation to the metamorphic foliation and the compositional banding of the schists and gneisses. Most usually they are decimeter to meter sized, rounded to elongated, and fractured bodies involved by the foliation. The major mineral is albite, more seldom graphic quartz, microcline, beryl, and pockets of muscovite and clinocllore can be found. The association of phlogopitization with the pegmatites is indicated by the observation that phlogopite schists are nearly monomineralic near the pegmatites while farther away they are hornblende bearing (Fig. 2). The amount of phlogopite increases and that of amphibole decreases towards the pegmatites. The emerald-bearing phlogopite schist constitutes coarse grained, strongly foliated and easily disaggregated decimeter to meter thick layers and pods enclosing quartz \pm feldspar veins. Talc appears along fault surfaces oriented parallel to the metamorphic foliation. Quartz and fluorite are secondary minerals that were introduced into the phlogopitite during the metassomatic transformation. It is worthwhile to note that quartz is absent in samples that contain Mg-hornblende besides phlogopite, possibly because this rock type was less transformed during metasomatism than the phlogopitite, as is also indicated by relics of Al-rich chromite preserved from the original ultramafic rock.

Emerald occurs in the phlogopitite and in the quartz veins as porphyroblasts which are sometimes bent or fractured. Centimeter to decimeter thick veins composed of quartz, feldspar, or quartz plus feldspar are found in the phlogopite schist. The quartz veins appear farther away from the pegmatites and contain the best-colored emerald crystals. In the feldspathic veins the emerald crystals are less well formed, commonly showing corroded outlines.

MATERIAL AND METHODS

The studied rock sample (Sample PI-5) is a phlogopite-plagioclase-hornblende schist belonging to the subterranean emerald mineralized zone in the Piteiras mine. The sample was chosen for geochronology due to two characteristics:

1. the presence of abundant metamorphic titanite surrounding ilmenite relics (Fig. 3), suggesting that titanite was formed during the same tectonometamorphic event responsible for the generation of the schist; and

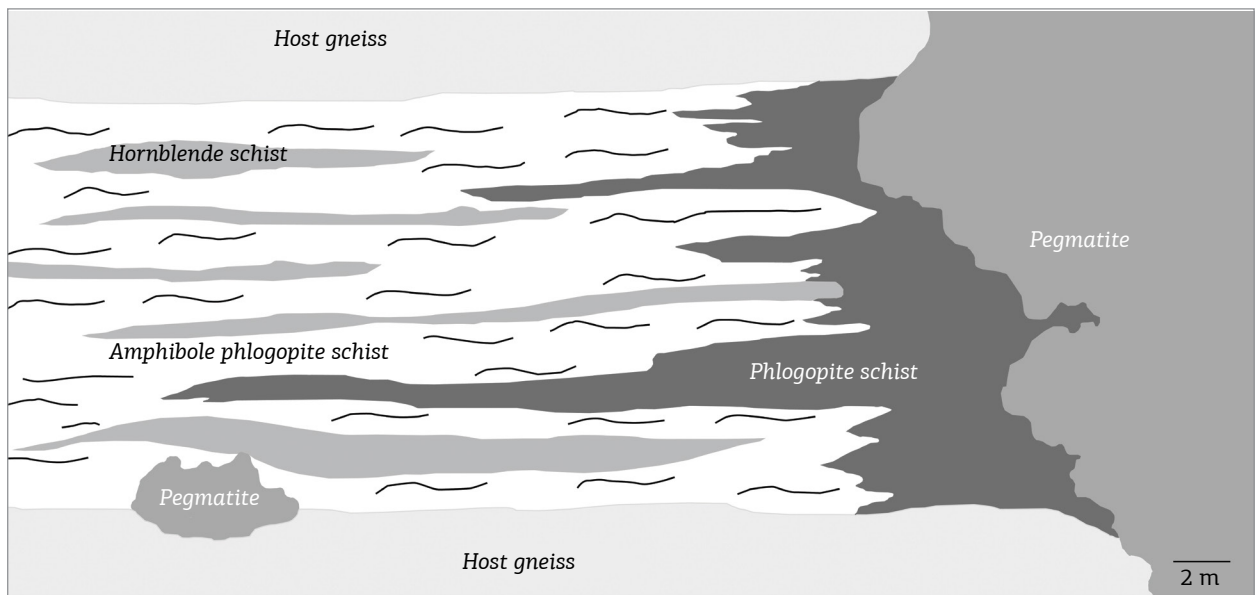


Figure 2. Schematic illustration showing the location of an emerald-bearing phlogopite schist adjacent to a pegmatite body in the Piteiras Mine (Viana 2004).

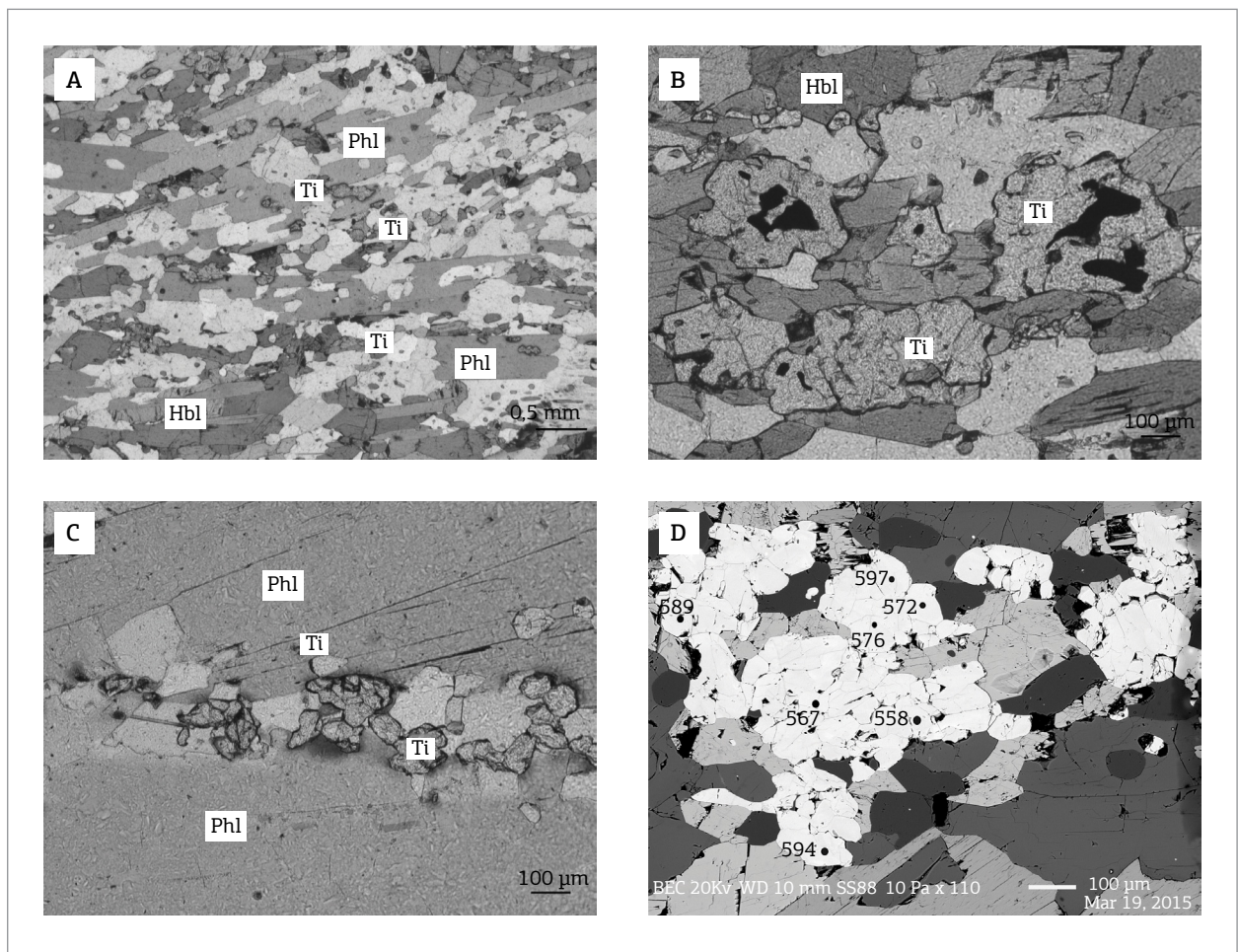


Figure 3. Photomicrographs (A – C) of thin section of the dated metamafic schist under plane polarized light. (A) General view showing titanite (grains with high relief), phlogopite, Mg-hornblende, plagioclase, and quartz (both colorless). (B) Ilmenite (black) surrounded by titanite. (C) Titanite grains surrounded by pleochroic haloes in phlogopite. (D) Ages (in million years) of titanite grains plotted on BSE-image. Ti = titanite; Phl = phlogopite; Hbl = Mg-hornblende.

2. the unusual high fluorine content (Table 1) in the titanite that was probably derived from the Borrachudos granites that were also the source of the Be for the emerald generation.

Thin sections were described on a Leica DM EP microscope at the Departamento de Geologia (DEGEO), Universidade Federal de Ouro Preto. Microprobe analyses on the titanite were performed on a JEOL microprobe JXA 8900 RL, at the Laboratório de Microanálises of the Universidade Federal de Minas Gerais, Belo Horizonte, Brazil. Operating conditions were 20 kV, 10 μm beam, and counting time of 100 s. The LA-ICP-MS analyses were performed using a Thermo Scientific Element II and a 213 nm CETAC laser at the isotope/geochemistry laboratory of the Department of Geology, Universidade Federal de Ouro Preto. The analyses were performed on a conventional polished (30 μm -thick) thin section. Sample contamination is excluded because the thin section was as clean as any other epoxy mount and 100% free of common Pb. In addition, the analyzed titanite grains were mostly larger than 200 μm whereas the laser holes were narrow (20 μm -wide) and substantially shallow (less than 5 μm -deep). Acquisitions consisted of 20 s measurement of the gas blank, followed by 20 s measurement of U, Th, and Pb signals during ablation, and 20 s washout. Laser conditions were 20 μm beam at 10 Hz and 0.02 J energy, giving a fluency of 8 J/mm. Common Pb corrected isotopic ratios were reduced using an Excel spreadsheet (Gerdes & Zeh 2006). Apparent age calculations and concordia diagrams were produced using Isoplot 4 (Ludwig 2012).

Two standards were used during runs: the primary standard BLR (1049.9 ± 1.3 Ma; Aleinikoff *et al.* 2007) and the secondary standard Khan titanite (522.2 ± 2.2 Ma, Heaman 2009). Twenty-five within-run analyses of the secondary standard gave a concordia age of 524 ± 2.6 Ma whereas six analyses of BLR (as secondary standard) gave a concordia age of 1053 ± 10 Ma (Table 2).

RESULTS

Petrography

Sample PI-5 comes from an amphibolite facies metamafic schist (Fig. 3A) of the mineralized zone at the Piteiras mine. It is composed of Mg-hornblende (40 vol.%), phlogopite (25 vol.%), plagioclase (23 vol.%), quartz (7 vol.%), and titanite (5 vol.%). There is a mineralogical layering with hornblende-rich layers alternating with phlogopite-rich ones. Titanite (Fig. 3A – C) is more abundant in the phlogopite-rich layers, where it may reach about 10 vol.%. Ilmenite is a relict accessory mineral being always surrounded by titanite (Fig. 3B).

Fluorine-aluminum-bearing titanite

In metamafic rocks of the mineralized zone from the Piteiras mine, Al-rich titanite commonly constitutes 0.5 – 1 mm large clusters that may surround ilmenite relics (Fig. 3B). Titanite is characterized by relatively low interference colors of upper second to lower third order and for

Table 1. Chemical composition (wt.%) by microprobe analyses of fluorine-aluminum-bearing titanite from the Piteiras mine.

	SiO ₂	TiO ₂	Al ₂ O ₃	FeO	MnO	CaO	F	Sum
PI5-Ca-Tit-1	31.48	28.76	8.01	0.75	0.08	28.60	2.39	100.07
PI5-Ca-Tit-2	31.42	27.59	8.96	0.55	0.13	29.13	2.86	100.64
PI5-Ca-Tit-3	31.32	31.14	6.45	0.69	0.11	29.02	2.38	101.11
PI5-Ca-Tit-4	31.18	28.28	8.35	0.67	0.11	29.06	2.84	100.49
PI5-Ca-Tit-5	31.21	29.64	7.45	0.82	0.15	28.80	2.21	100.28
PI5-Ca-Tit-6	30.86	29.27	7.47	0.72	0.15	28.53	2.64	99.64
PI5-Ca-Tit-7	30.68	27.87	8.38	0.56	0.11	28.69	2.09	98.38
PI5Ca-C1-Tit-8	30.34	27.80	8.34	0.63	0.05	28.30	1.84	97.30
PI5Ca-C1-Tit-9	30.67	28.93	7.47	0.71	0.15	28.11	2.16	98.20
PI5Ca-C1-Tit-10	31.15	28.16	7.89	0.68	0.09	28.35	2.49	98.81
PI5Ca-C1-Tit-11	30.87	29.10	7.26	0.70	0.10	28.37	2.66	99.06
PI5Ca-C1-Tit-12	30.56	29.95	7.19	0.66	0.06	28.54	1.67	98.63

Table 2. Results of U-Pb LA-ICP-MS dating of titanite from the Piteiras mine in the Itabira-Nova Era Emerald District.

Spot	²⁰⁷ Pb (cps)	²³⁵ U (ppm)	²⁰⁸ Pb (ppm)	²³² Th/U	²⁰⁶ Pb (%)	²⁰⁷ Pb 235U	±2s (%)	²⁰⁶ Pb 238U	±2s (%)	rhoe	²⁰⁷ Pb 206Pb	±2s (%)	²⁰⁶ Pb 238U	±2s (Ma)	²⁰⁷ Pb 235U	±2s (Ma)	²⁰⁷ Pb 206Pb	±2s (Ma)	Conc %
Sample PI-5																			
4sSMPABC056	4910	19.00	1.96	0.06	0.255	0.731	2.770	0.091	2.279	0.823	0.059	1.574	559	12	557	12	550	34	101.65
4sSMPABC055	4893	19.62	2.06	0.06	0.074	0.746	3.036	0.092	2.520	0.830	0.059	1.693	568	14	566	13	558	37	101.85
4sSMPABC030	466	2.50	0.26	0.01	0.954	0.844	6.658	0.104	4.507	0.677	0.059	4.901	637	27	621	31	566	107	112.59
4sSMPABC016	486	3.41	0.31	0.01	1.128	0.730	6.987	0.090	4.776	0.684	0.059	5.099	554	25	556	30	568	111	97.56
4sSMPABC078	883	2.20	0.20	0.01	2.045	0.740	5.216	0.090	3.363	0.645	0.060	3.988	556	18	562	23	587	87	94.84
4sSMPABC026	500	2.26	0.21	0.01	1.553	0.749	6.495	0.091	4.019	0.619	0.060	5.102	562	22	568	29	591	111	95.19
4sSMPABC013	496	4.29	0.41	0.01	0.118	0.801	6.101	0.097	3.760	0.616	0.060	4.805	598	22	597	28	595	104	100.42
4sSMPABC082	849	1.84	0.17	0.01	0.572	0.754	4.551	0.091	3.209	0.705	0.060	3.226	563	17	570	20	598	70	94.15
4sSMPABC034	707	2.82	0.26	0.01	0.797	0.783	4.908	0.095	3.205	0.653	0.060	3.717	583	18	587	22	605	80	96.35
4sSMPABC032	463	1.96	0.19	0.01	1.986	0.794	6.064	0.096	3.506	0.578	0.060	4.948	590	20	593	28	605	107	97.55
4sSMPABC011	723	5.88	0.56	0.01	1.524	0.778	5.175	0.094	3.600	0.696	0.060	3.718	579	20	584	23	606	80	95.48
4sSMPABC070	1198	2.92	0.26	0.01	2.526	0.745	4.427	0.090	2.660	0.601	0.060	3.539	555	14	565	19	607	77	91.52
4sSMPABC081	675	1.30	0.12	0.01	1.940	0.753	6.115	0.091	3.547	0.580	0.060	4.981	560	19	570	27	608	108	92.20
4sSMPABC084	27029	35.25	3.77	0.03	1.995	0.751	3.559	0.091	2.849	0.801	0.060	2.133	559	15	569	16	608	46	92.01
4sSMPABC017	687	3.89	0.36	0.01	2.403	0.767	5.206	0.092	3.012	0.579	0.060	4.246	570	16	578	23	611	92	93.35
4sSMPABC079	617	1.12	0.10	0.01	2.846	0.746	6.715	0.090	4.664	0.695	0.060	4.831	555	25	566	30	611	104	90.71
4sSMPABC053	27553	63.13	6.82	0.03	2.105	0.772	3.328	0.093	2.469	0.742	0.060	2.231	572	14	581	15	615	48	93.10
4sSMPABC075	1037	2.63	0.25	0.01	1.591	0.787	4.639	0.095	2.680	0.578	0.060	3.786	583	15	590	21	615	82	94.81
4sSMPABC033	653	2.08	0.20	0.01	3.521	0.760	6.130	0.091	3.272	0.534	0.060	5.184	563	18	574	27	615	112	91.60
4sSMPABC052	27073	61.98	6.78	0.03	2.123	0.779	3.568	0.094	2.757	0.773	0.060	2.266	577	15	585	16	616	49	93.67
4sSMPABC083	801	1.41	0.13	0.01	2.043	0.751	5.885	0.090	3.782	0.643	0.060	4.509	557	20	569	26	618	97	90.16
4sSMPABC022	760	3.77	0.36	0.01	1.282	0.780	4.898	0.094	3.430	0.700	0.060	3.496	577	19	586	22	620	75	93.05
4sSMPABC031	703	2.59	0.24	0.01	2.487	0.786	5.089	0.094	2.895	0.569	0.060	4.186	581	16	589	23	607	90	95.71
4sSMPABC080	684	1.29	0.12	0.01	0.707	0.775	5.325	0.093	4.081	0.566	0.058	3.421	572	22	583	24	532	74	107.46
4sSMPABC054	28288	63.08	6.96	0.03	2.034	0.802	3.624	0.096	2.912	0.803	0.060	2.158	589	16	598	17	594	46	99.20
4sSMPABC050	27572	64.55	7.33	0.03	2.180	0.809	3.541	0.096	2.684	0.758	0.059	2.310	594	15	602	16	556	50	106.73
4sSMPABC096	710	0.89	0.08	0.01	3.097	0.765	5.942	0.091	3.491	0.588	0.061	4.808	562	19	577	26	633	104	88.84
4sSMPABC051	27430	62.79	7.13	0.03	1.972	0.814	3.412	0.097	2.679	0.585	0.060	2.112	596	15	605	16	607	45	98.25
4sSMPABC014	632	3.87	0.37	0.01	2.482	0.800	6.095	0.095	4.238	0.695	0.061	4.381	586	24	597	28	638	94	91.85
4sSMPABC025	632	2.58	0.25	0.01	2.469	0.802	6.090	0.095	4.238	0.696	0.060	4.374	586	24	598	28	607	94	96.49
4sSMPABC095	608	0.66	0.06	0.01	3.756	0.762	6.166	0.090	3.783	0.583	0.059	4.869	557	20	575	27	578	105	96.26
4sSMPABC015	510	2.49	0.26	0.01	3.866	0.804	6.671	0.095	4.615	0.592	0.060	4.818	584	26	599	31	588	103	99.31
4sSMPABC029	510	1.61	0.17	0.01	3.853	0.806	6.666	0.095	4.615	0.692	0.059	4.810	584	26	600	31	556	103	104.92
4sSMPABC073	583	0.95	0.10	0.01	4.340	0.788	5.845	0.092	4.257	0.728	0.058	4.005	567	23	590	26	534	86	106.24
4sSMPABC012	529	2.77	0.29	0.01	4.408	0.834	6.198	0.097	4.484	0.723	0.059	4.279	595	26	616	29	550	91	108.35
4sSMPABC097	32324	36.12	4.34	0.03	2.601	0.897	3.431	0.104	2.382	0.694	0.060	2.470	636	14	650	17	593	53	107.26

Continue...

Titanite geochronology emerald Itabira

Table 2. Continuation.

Spot	^a 207Pb (cps)	^b U (ppm)	^b Pb (ppm)	^b Th/U	^c 206Pb (%)	^d 207Pb/235U	^{±2s} (%)	^d 206Pb/238U	^{±2s} (%)	rhoe	^d 207Pb/206Pb	^{±2s} (%)	206Pb/238U	^{±2s} (Ma)	207Pb/235U	^{±2s} (Ma)	207Pb/206Pb	^{±2s} (Ma)	Conc %
Khan Accepted age 522 Ma																			
Within run standard points normalized with BLR 1																			
4.sSMPABC094	4852	10.38	1.00	0.06	0.000	0.668	2.986	0.084	2.512	0.841	0.058	1.614	521	13	520	12	516	35	100.90
4.sSMPABC093	4891	9.95	0.96	0.06	0.410	0.674	2.784	0.084	2.318	0.833	0.058	1.542	522	12	523	11	529	34	98.60
4.sSMPABC092	4827	10.47	1.03	0.06	0.000	0.689	2.649	0.086	2.252	0.850	0.058	1.395	532	12	532	11	535	31	99.32
4.sSMPABC091	4933	10.56	1.03	0.06	0.352	0.684	2.985	0.085	2.487	0.833	0.058	1.652	527	13	529	12	539	36	97.70
4.sSMPABC090	4950	10.74	1.04	0.06	0.000	0.668	2.499	0.084	2.047	0.819	0.058	1.435	518	10	519	10	523	31	99.13
4.sSMPABC089	25842	28.78	2.88	0.03	2.114	0.688	3.652	0.084	2.862	0.784	0.059	2.269	519	14	531	15	585	49	88.74
4.sSMPABC086	30209	35.11	3.61	0.03	2.875	0.700	3.862	0.085	2.684	0.695	0.060	2.777	526	14	539	16	594	60	88.57
4.sSMPABC084	799	1.21	0.11	0.01	3.453	0.678	5.969	0.082	3.855	0.646	0.060	4.557	510	19	525	25	593	99	86.06
4.sSMPABC067	989	1.60	0.14	0.01	4.463	0.705	6.089	0.084	3.603	0.592	0.061	4.909	522	18	542	26	629	106	82.98
4.sSMPABC066	934	2.02	0.18	0.01	1.712	0.684	5.093	0.084	2.945	0.578	0.059	4.154	517	15	529	21	582	90	88.85
4.sSMPABC062	738	1.78	0.16	0.01	2.813	0.691	6.186	0.085	4.156	0.672	0.059	4.582	525	21	533	26	570	100	92.00
4.sSMPABC068	5148	16.60	1.54	0.06	0.000	0.660	2.486	0.081	2.089	0.840	0.059	1.348	505	10	515	10	560	29	90.14
4.sSMPABC067	5439	20.51	2.03	0.06	0.000	0.690	2.726	0.086	2.353	0.863	0.058	1.376	534	12	533	11	527	30	101.27
4.sSMPABC021	6311	43.67	4.33	0.06	0.000	0.685	3.212	0.086	2.865	0.892	0.058	1.452	531	15	530	13	525	32	101.21
4.sSMPABC020	6258	45.30	4.48	0.06	0.764	0.680	3.091	0.085	2.486	0.804	0.058	1.837	529	13	527	13	518	40	102.04
4.sSMPABC019	6036	45.36	4.53	0.06	0.000	0.680	3.094	0.086	2.745	0.887	0.058	1.428	529	14	527	13	518	31	102.10
4.sSMPABC018	6737	52.01	5.12	0.06	0.000	0.681	3.430	0.085	3.190	0.930	0.058	1.260	528	16	527	14	524	28	100.72
4.sSMPABC010	6244	73.33	7.35	0.06	0.000	0.696	3.228	0.087	2.872	0.890	0.058	1.473	537	15	536	14	531	32	101.25
4.sSMPABC009	6258	78.25	7.74	0.06	0.764	0.680	3.091	0.085	2.486	0.804	0.058	1.837	529	13	527	13	518	40	102.04
4.sSMPABC008	6092	80.12	7.94	0.06	0.000	0.673	3.075	0.085	2.728	0.887	0.058	1.421	524	14	522	13	514	31	101.99
4.sSMPABC007	6737	92.46	9.11	0.06	0.000	0.681	3.430	0.085	3.190	0.930	0.058	1.260	528	16	527	14	524	28	100.69
4.sSMPABC006	6406	94.36	9.38	0.06	0.000	0.687	3.437	0.086	3.143	0.914	0.058	1.391	532	16	531	14	524	31	101.52
4.sSMPABC004	6418	107.70	10.67	0.06	0.000	0.676	3.037	0.085	2.772	0.913	0.058	1.241	526	14	524	13	517	27	101.83
4.sSMPABC003	6216	114.69	11.20	0.06	0.000	0.665	3.270	0.084	2.989	0.914	0.057	1.325	519	15	518	13	510	29	101.93

BLR 1 Accepted age 1049 Ma

Within run standard points normalized with BLR 1

4.sSMPABC001	44702	382.30	75.32	0.03	1.012062	1.868	2.405	0.180	2.001	0.832	0.075	1.334	1065	20	1070	16	1080	27	98.66
4.sSMPABC002	41961	514.18	99.92	0.03	0.756406	1.839	2.048	0.178	1.804	0.881	0.075	0.969	1057	18	1059	14	1064	19	99.35
4.sSMPABC003	42130	409.02	79.60	0.03	0.694349	1.837	2.051	0.178	1.809	0.882	0.075	0.968	1057	18	1059	14	1062	19	99.52
4.sSMPABC004	42274	446.58	86.57	0.03	0.722678	1.810	2.112	0.177	1.815	0.860	0.074	1.079	1053	18	1049	14	1040	22	101.24
4.sSMPABC005	42275	474.94	90.49	0.03	0.675464	1.769	2.004	0.174	1.759	0.878	0.074	0.961	1032	17	1034	13	1039	19	99.35

^aWithin run background-corrected mean ²⁰⁷Pb signal in cps (counts per second); ^bU and Pb content and Th/U ratio were calculated relative to BLR reference STD; ^cpercentage of the common Pb on the ²⁰⁶Pb. b.d. = below detection limit; ^dcorrected for background. within-run Pb/U fractionation (in case of 206Pb/238U) and common Pb using Stacy and Kramers (1975) model Pb composition and subsequently normalised to GJ-1 (ID-TIMS value/measured value); ²⁰⁷Pb/²³⁵U calculated using ²⁰⁷Pb/²⁰⁶Pb/(²³⁸U/²⁰⁶Pb*1/1.37.88); ^erho is the ²⁰⁶Pb/²³⁸U/²⁰⁷Pb/²³⁵U error correlation coefficient.

being surrounded by strong pleochroic haloes when included in phlogopite (Fig. 3C). Chemical analyses by electron microprobe show relatively high contents of Al₂O₃ (7.19 – 8.96 wt.%, Table 1) and fluorine (around 2 wt.%). Due to the high Al content, this titanite was classified as grothite (Gaines *et al.* 1997) by Delgado *et al.* (2005).

Geochronology

Figure 3D is a BSE image of the sample PI-5, showing bright white titanite clusters with the location of some dated points. The mineral with light gray color is Mg-hornblende and the dark gray ones are plagioclase and quartz. The sample consists of Mg-hornblende, phlogopite, plagioclase, quartz, and titanite and is marked by a strong foliation defined by hornblende and phlogopite. Note that titanite is part of this fabric indicating growth during the metamorphic event.

Thirty-six analyses were performed on center and rims of the titanite grains (Table 2). No age difference could be detected between center and rim of titanite grains. Pooling of all data points did not yield a concordia age (Fig. 4). The points scatter about a mean ²⁰⁶Pb/²³⁸U age of 576 ± 7 Ma

which is considered the age of titanite growth during medium-grade metamorphism.

DISCUSSION AND CONCLUSIONS

The substitution of Ti by Al in titanite, as found in the dated fluorine-aluminum-bearing titanite, can be the result of the high activity of fluorine that causes the simultaneous substitution of O by (F, OH) (Černý & Povondra 1972). Thereafter, the discussions regarding the formation of the titanite must take into consideration the source of fluorine, which is a scarce element in mafic igneous rocks but relatively abundant in granitic rocks. The metamafic schist belongs to the Archean Metavolcanosedimentary Sequence that surrounds the 1.7 Ga anorogenic Borrachudos metagranites. The Borrachudos metagranites postdate the main deformation phases of the 2.2 – 2.0 Paleoproterozoic Transamazonian tectonothermal event. The origin of fluorine must be linked to these granitic intrusions and their pegmatites which were also the source of beryllium for the emerald found in the associated phlogopite schists. The generation of emerald as well

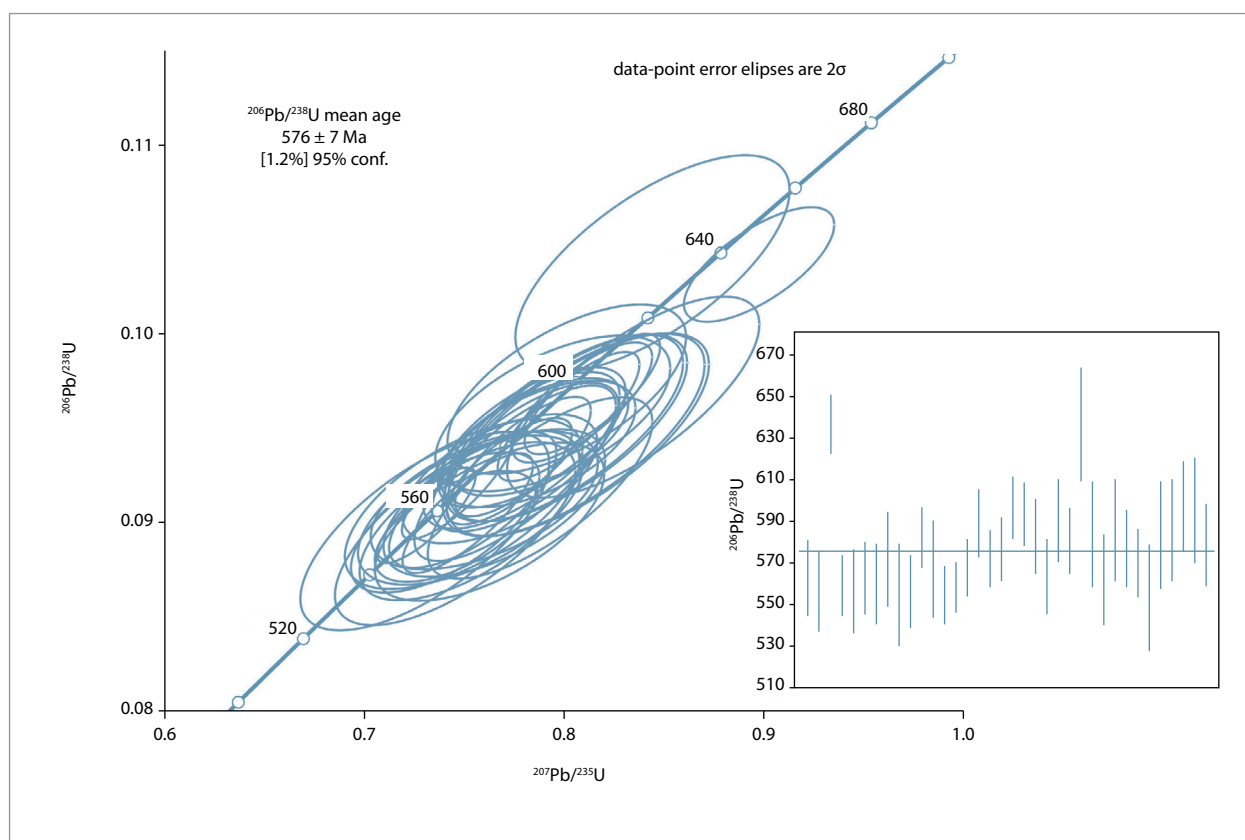


Figure 4. U-Pb concordia and weighed mean diagrams of LA-ICP-MS analyses of fluorine-aluminum-bearing titanite from a metamafic schist of the Piteiras mine.

as the titanite was possibly due to the metassomatic introduction of, respectively, Be and F into the metaultramafic and metamafic rocks. The discussions on the age of titanite and emerald must also take into consideration the nature of the rocks where the two minerals are found: These rocks are strongly deformed and completely metamorphosed and transformed by metassomatic reactions. As discussed in the literature (Grundmann & Morteani 1989, Franz *et al.* 1996, Franz & Morteani 2002), the formation of schist-type emerald deposits such as that of the Piteiras mine involves a tectonometamorphic event that supplies the necessary heat and fluids to enhance the metassomatic reactions between the granitic and the ultramafic rocks. Since the plausible source of beryllium and fluorine are the postorogenic Borrachudos metagranites and pegmatites, the only younger tectonometamorphic event that could have been responsible for the deformation, metamorphism, and metassomatic reactions between the Be/F-bearing and the Cr-bearing rocks was the 0.7 – 0.5 Ga Neoproterozoic Brasiliano event, which is the last tectonothermal event registered in the region. The obtained 576 ± 7 Ma age of the dated titanite corroborates the interpretation that the Brasiliano event was indeed responsible for its generation.

We conclude thereafter that the 576 ± 7 Ma age of the fluorine-aluminum-bearing titanite of the metamafic rock associated with the emerald-mineralized phlogopite schists in the Piteiras mine from the Itabira-Nova Era Emerald District could also be the age of the emerald generation

during the Neoproterozoic tectonometamorphic Brasiliano event. We suggest that the following geological processes were involved in the generation of the emerald deposits from the Itabira-Nova Era region:

1. Formation of the Volcanosedimentary Sequence (including Cr-bearing ultramafic rocks) of the Guanhães Complex during the Archean (~ 2.8 Ga).
2. Generation and metamorphism of the gneisses of the Mantiqueira Complex during the Paleoproterozoic Transamazonian event (2.2 – 2.0 Ga) and intrusion of the late 1.7 Ga anorogenic Borrachudos granite and their pegmatites.
3. Regional metamorphism during the Neoproterozoic and generation of the schist-type emerald mineralization by reactions between Be-bearing granites and pegmatites and Cr-rich metaultramafic rocks was enhanced by deformation and heat supplied by the tectonometamorphic Brasiliano event (~ 0.7 – 0.5 Ga). The participation of hydrothermal fluids was crucial for the growth of emerald as well as for the phlogopitization of the ultramafic rock.

ACKNOWLEDGMENTS

Hanna Jordt-Evangelista acknowledges the support from FAPEMIG (APQ-00732-12). Cristiano Lana acknowledges the support from FAPEMIG (CRA 03943/10 and 067-10).

REFERENCES

- Aleynikoff J.N., Wintsch R.P., Tollo R.P., Unruh D.M., Fanning C.M., Schmitz M.D. 2007. Ages and origins of rocks of Killingworth dome, South-Central Connecticut: Implications for the tectonic evolution of southern New England. *American Journal of Science*, **307**(1):63-118.
- Alkmim F.F. & Marshak S. 1998. Transamazonian orogeny in the Southern São Francisco Craton region, Minas Gerais, Brazil: evidence for Paleoproterozoic collision and collapse in the Quadrilátero Ferrífero. *Precambrian Research*, **90**(1-2):29-58.
- Almeida, F.F.M. 1977. O Cráton do São Francisco. *Revista Brasileira de Geociências*, **7**:349-364.
- Brito Neves B.B., Cordani U.G. 1991. Tectonic evolution of South America during the late Proterozoic. *Precambrium Research*, **53**(1-2):23-40.
- Černý P. & Povondra P. 1972. An Al, F-rich metamict titanite from Czechoslovakia. *Neues Jahrbuch für Mineralogie Monatshefte*, 400-406.
- Chemale Jr. F. 1987. Gênese das rochas graníticas do tipo Borrachudos. In: Congresso Brasileiro de Geoquímica, 1. *Anais...*, **1**:171-186.
- Chemale Jr. F., Quade H., Van Schmus W.R. 1997. Petrography, geochemistry and geochronology of the Borrachudo and Santa Bárbara metagranites, Quadrilátero Ferrífero, Brazil. *Zentralblatt für Geologie und Paläontologie, Teil I*, **3**(6):739-750.
- Correia Neves J.M., Soares, A.C.P., Marciano, V.R.P.R.O. 1986. A Província Pegmatítica do Brasil à luz dos conhecimentos atuais. *Revista Brasileira Geociências*, **16**(1):106-118
- Delgado C.E.R. 2007. *Geologia e petrogênese na região da Província Esmeraldífera de Itabira, MG*. MS Dissertation, Departamento de Geologia, Universidade Federal de Ouro Preto, Ouro Preto, 130 p.
- Delgado C.E.R., Jordt-Evangelista H., Viana D.J. 2005. Grothita (titanita de Alto Al) da Província Esmeraldífera de Itabira, MG. In: 9º Simpósio de Geologia do Sudeste e 13º Simpósio de Geologia de Minas Gerais. *Anais...*, p. 77.
- Dorr J.V.N. 1969. *Physiographic, stratigraphic and structural development of the Quadrilátero Ferrífero Minas Gerais, Brazil*. U.S. Geological Survey. Washington, 110 p. (Professional Paper 641-A).
- Dorr J.V.N. & Barbosa, A.L.M. 1963. *Geology and ore deposits of the Itabira District, Minas Gerais, Brazil*. U.S. Geological Survey. Washington, 110 p. (Professional Paper 341-C).
- Dossin I.A., Dossin T.M., Charvet J., Cocherie A., Rossi P. 1993. Single-zircon dating by step-wise Pb-evaporation of Middle Proterozoic magmatism in the Espinhaço Range, Southeastern São Francisco Craton (Minas Gerais, Brazil). In: Simpósio do Cráton do São Francisco, 2. *Anais...*, 39-42.

- Dussin T.M., Dussin I.A., Noce C.M., Rossi P., Charvet J. 1997. Tectonic setting and origin of the Mesoproterozoic Borrachudos granites (MG, Brazil). In: South-American Symposium on Isotope Geology, Campos do Jordão, Brazil. *Extended Abstracts*, 104-106.
- Fernandes M.L.S., Marciano V.R.P.R.O., Oliveira R.C., Correia Neves J.M., Dilácio M.V. 1995. Granitos Borrachudos: um exemplo de granitogênese anorogênica na Porção Central do Estado de Minas Gerais. *Geonomos*, **2**(2): 23-29.
- Fernandes M.L.S., Pedrosa Soares A.C., Noce C.M., Widemann C., Correia Neves J.M. 2000. U-Pb geochronology of the Borrachudos Suite: Evidence of Brasiliano tectonism recorded by late Paleoproterozoic anorogenic granites (Araçuaí Belt, Minas Gerais, Brazil). In: International Geological Congress. *Abstracts*. CD-ROM, Abstract G1803074.
- Franz G. & Morteani G. 2002. Be-Minerals: Synthesis, stability, and occurrence in metamorphic rocks. In: Grew E.S. (ed.). *Beryllium – Mineralogy, Petrology, and Geochemistry*. Reviews in Mineralogy and Petrology, **50**(1):551-589.
- Franz G., Gilg H.A., Grundmann G., Morteani, G. 1996. Metassomatism at a granitic pegmatite – Dunite contact in Galicia: the Franqueira occurrence of chrysoberyl (Alexandrite), Emerald, and Phenakite: discussion. *Canadian Mineralogist*, **34**:1329-1331.
- Gaines R.V., Skinner H.C.W., Foord E.E., Mason B., Rosenzweig A., King V.T., Dowty E. 1997. Titanite. In: Gaines R.V. et al. (eds.) *Dana's New Mineralogy*. New York, John Wiley, p. 1092-1094.
- Gerdes A., Zeh A. 2006. Combined U-Pb and Hf isotope LA-(MC)-ICP-MS analyses of detrital zircons: comparison with SHRIMP and new constraints for the provenance and age of an Armorican metasediment in Central Germany. *Earth and Planetary Science Letters*, **249**(1-2):47-61.
- Giuliani G., Silva L.J.H.D., Couto P. 1990. Origin of emerald deposits of Brazil. *Mineralium Deposita*, **25**:57-64.
- Grossi-Sad J.H., Chiod Filho C., Santos J.F., Magalhães, J.M.M., Carelos P.M. 1990. Duas suítes graníticas do bordo sudeste do Crátion Sanfranciscano em Minas Gerais: petroquímica e potencial metalogenético. In: SBG, Cong. Bras. Geol., 36, Natal, 1990. *Anais*, **4**: 1836-1848.
- Grundmann G. & Morteani G. 1989. Emerald mineralization during regional metamorphism: The Habachtal (Austria) and Leydsdorp (Transvaal, South Africa) deposits. *Economic Geology*, **84**(7):1835-1849.
- Heaman L.M. 2009. The application of U-Pb geochronology to mafic, ultramafic and alkaline rocks: an evaluation of three mineral standards. *Chemical Geology*, **261**(1-2):42-51.
- Jordt-Evangelista H., César-Mendes J., Lima A.L.C. 2000. Amazonitização em granito resultante da intrusão de pegmatitos. *Revista Brasileira de Geociências*, **30**(4):693-698.
- Ludwig K.R. 2012. *Isoplot/Ex Version 3.75: A Geochronological toolkit for Microsoft Excel*. Berkeley, CA, Berkeley Geochronology Center Special Publication 5, 72 p.
- Machado G.A.A. 1994. *Geologia da região e aspectos genéticos das jazidas de esmeralda de Capoeirana e Belmont, Nova Era - Itabira, MG*. MS Dissertation, Instituto de Geociências, Universidade de São Paulo, São Paulo, 134 p.
- Machado G.A.A. 1998. *Jazidas de esmeralda de Capoeirana e Belmont – MG: Geologia, petrogênese e metalogênese*. PhD Thesis, Instituto de Geociências, Universidade de São Paulo, São Paulo, 294 p.
- Morteani G., Preinfalk C., Horn A.H. 2000. Classification and mineralization potential of the pegmatites of the Eastern Brazilian Pegmatite Province. *Mineralium Deposita*, **35**:638-655.
- Netto C., Araújo M.C., Pinto C.P., Drumond J.B.V. 1998. Projeto Leste- Programa Levantamentos Geológicos Básicos do Brasil - Cadastramento de Recursos Minerais. Província Pegmatítica Oriental. Mapeamento Geológico e Cadastramento de Recursos Minerais da Região Leste de Minas Gerais, Belo Horizonte, CPRM, 105 p. (Relatório Final).
- Padilha A.V., Vieira V.S., Bruno E.M. 2000. Programa Levantamentos Geológicos Básicos do Brasil; Carta Geológica, Carta Metalogenética/Previsional - Escala 1:100.000 (Folha SE.23-Z-D-IV Itabira) Estado de Minas Gerais. Brasília, DNPM/CPRM. Mapa e texto explicativo.
- Paiva G. 1946. Províncias Pegmatíticas do Brasil. DNPM/DFPM, Boletim 78, p. 13-21
- Peres G.G., Alkmim FF., Jordt-Evangelista H. 2004. The Southern Araçuaí Belt and the Dom Silvério Group: geologic architecture and tectonic significance. *Anais da Academia Brasileira de Ciências*, **76**(4):771-790.
- Preinfalk C., Kostitsyn Y., Morteani G. 2002. The pegmatites of the Nova Era-Itabira-Ferros pegmatite district and the emerald mineralisation of Capoeirana and Belmont (Minas Gerais, Brazil): Geochemistry and Rb-Sr dating. *Journal of South American Earth Sciences*, **14**(8):867-887.
- Ribeiro P.A. 2006. *Geologia e controle estrutural dos corpos mineralizados em esmeraldas do Garimpo de Capoeirana, Nova Era/MG*. MS Dissertation, Departamento de Geologia, Universidade Federal de Ouro Preto, Ouro Preto, 128 p.
- Ribeiro-Althoff A.M., Cheilletz A., Giuliani G., Féraud G., Barbosa-Camacho G., Zimmermann J.L. 1997. ⁴⁰Ar/³⁹Ar and K-Ar geochronological evidence for two periods (~2 Ga and 650 to 500 Ma) of emerald formation in Brazil. *International Geology Review*, **39**(10):924-937.
- Schorscher H.D. 1991. Quadrilátero Ferrífero e Espinhaço Meridional. In: 3º Congresso Brasileiro Geoquímica. São Paulo, *Guia de Excursão*, p. 37-87.
- Schwarz D. & Giuliani G. 2001. Emerald deposits – a review. *Australian Gemologist*, **21**:17-23.
- Schwarz, D., Giuliani, G., Grundman, G., Glass, M. 2002. The origin of emerald. In: *Emeralds of the World*, extraLapis English, **2**: 18-23.
- Silva L.C., Armstrong R. Noce C.M., Carneiro M.A., Pimentel M., Pedrosa-Soares A.C., Leite C.A., Vieira V.S., Silva M.A., Paes V.J.C., Cardoso Filho J.M. 2002. Reavaliação da evolução geológica em terrenos pré-cambrianos brasileiros com base em novos dados U-Pb SHRIMP, Parte II: Orógeno Araçuaí, Cinturão Mineiro e Crátion São Francisco Meridional. *Revista Brasileira de Geociências*, **32**(4):513-528.
- Souza J.L. 1988. *Mineralogia e geologia da esmeralda da Jazida de Itabira - Minas Gerais*. MS Dissertation, Instituto de Geociências, Universidade de São Paulo, São Paulo, 192 p.
- Souza J.L., César-Mendes J., Bello R M S., Svisero D.P., Valarelli J.V. 1992. Petrographic and microthermometrical studies of emeralds in the garimpo de Capoeirana, Nova Era, Minas Gerais State, Brazil. *Mineralium Deposita*, **27**(2):161-168.
- Viana D.J. 2004. *Geologia e petrogênese da jazida de esmeralda de Piteiras, MG*. MS Dissertation, Departamento de Geologia, Universidade Federal de Ouro Preto, Ouro Preto, 220 p.
- Viana D.J., Jordt-Evangelista H., Souza Gomes C. 2006. Esmeralda da Mina de Piteiras, região de Itabira, MG: geologia e gênese. *Revista Brasileira de Geociências*, **36**: 174-178.